1-1-2014

Effects of organic and colloidal fouling on the rejection of two pharmaceutically active compounds (PhACs) by nanofiltration processes: role of membrane foulants

Long D. Nghiem
University of Wollongong, longn@uow.edu.au

Christiane Espendiller
University of Wollongong, ce498@uowmail.edu.au

Effects of organic and colloidal fouling on the rejection of two pharmaceutically active compounds (PhACs) by nanofiltration processes: role of membrane foulants

Publication Details

Nghiem, L. D. & Espendiller, C. (2014). Effects of organic and colloidal fouling on the rejection of two pharmaceutically active compounds (PhACs) by nanofiltration processes: role of membrane foulants. Desalination and Water Treatment, 52 (4-6), 633-642.

Effects of organic and colloidal fouling on the rejection of two pharmaceutically active compounds (PhACs) by nanofiltration processes: Role of membrane foulants

Revised Manuscript Submitted to

Desalination and Water Treatment

March 2013

Long Duc Nghiem* and Christiane Espendiller

[1] School of Civil Mining and Environmental Engineering
The University of Wollongong, NSW 2522, Australia

* Corresponding author: Long Duc Nghiem, Email: longn@uow.edu.au, Ph +61 2 4221 4590

Abstract: Results reported here indicate that membrane fouling could influence the removal of two pharmaceutically active compounds (PhACs) namely – sulfamethoxazole and carbamazepine – by a nanofiltration process. The effects of membrane fouling on solute rejection by the tight nanofiltration NF-90 membrane were quite negligible. In contrast, remarkable effects of membrane fouling on the rejection of both inorganic salts and PhACs were observed with the larger pore size NF-270 membrane. The effects of membrane fouling on solute rejection were strongly foulant–dependent. The three model foulants (sodium alginate, bovine serum albumin (BSA), and silica colloid) used in this study resulted in three distinctive modes of membrane fouling. Subsequently, these three modes of membrane fouling consistently showed different effects on the membrane separation efficiency. Inorganic colloidal fouling resulted in the most severe rejection decrease while causing the least permeate flux decline. This observed reduction in rejection could be attributed to the cake-enhanced concentration polarization phenomenon which was also thought to be the primary mechanism of flux decline in inorganic colloidal fouling. In contrast, organic fouling caused by the model foulant alginate led to a lesser decrease in the rejection of PhACs despite the fact that alginate caused the most severe flux decline.

Keywords: nanofiltration, membrane fouling, pharmaceutically active compounds (PhACs), water recycling, proteins, colloidal particles, polysaccharides.

1 Introduction

The many worldwide problems associated with the lack of clean water are well known [1]. In many cases, potable water scarcity has also been seen as a major obstacle for economic growth. A strategic approach to addressing water shortages is the augmentation of environmental supplies by the reclaimed effluents using advanced water treatment technologies including high-pressure membrane processes such as reverse osmosis (RO) and nanofiltration (NF) [1-2]. In fact, most potable water recycling schemes utilize RO or NF membranes as a major physical barrier to remove contaminants of concern. At the centre of these contaminants are micropollutants such as pharmaceutically active compounds (PhACs), endocrine disrupting compounds, and industrial chemicals, which are known to be widespread in raw sewage and secondary treated effluent at trace levels. Their occurrence in treated municipal wastewater effluents and sewage impacted water bodies at μg/L level or lower is wide spread in many parts of the world [3]. The risk of trace level occurrences of such micropollutants is however still largely unknown [3]. Thus, a major limiting factor impeding the rates of water recycling is our capacity to treat secondary effluent to a high standard suitable for a range of potable and near potable reuse applications.

Eminent with the focus on micropollutant removal from wastewater, NF/RO membrane filtration is an effective and reliable technology to address this issue. Numerous dedicated studies have been conducted to evaluate the removal efficiency of micropollutants by NF/RO membranes in laboratory and full scale installations. Several attempts have also been made to investigate the performance of NF/RO membranes under various operating conditions (e.g. solution pH, ionic strength, permeate flux, and the presence of natural organic matter) [4-8]. These studies have highlighted the complexity of the removal mechanisms involved. In fact, it has been established that membrane characteristics, physiochemical properties of the solute as well as chemistry of the feed solution can all play an important role in governing the separation process of micropollutants by NF/RO membranes [9]. Given the already extensive use of NF/RO membranes in both drinking water and water recycling applications, recent research has also revealed an urgent need to assess the long term effects of membrane fouling the rejection of micropollutants. Indeed, membrane fouling is an inevitable problem in full scale NF/RO installations due to the presence of organic and particulate matter, microorganisms and sparingly

soluble salts in the feed water [10]. These components are ubiquitous in secondary treated effluent and can be responsible for four distinctive modes of membrane fouling namely organic fouling, colloidal fouling, bio-fouling, and scaling, respectively [10]. Although data addressing this important aspect of NF/RO filtration remain rather scarce, information available to date indicated that the fouling layer can considerably alter the separation behavior of micropollutants, leading to either an increase or a decrease in rejection as compared to the virgin (clean) membrane condition [11-13].

The underlying mechanisms of the effects of membrane fouling on micropollutant rejection have been linked to the membrane pore size and physiochemical properties of the solutes [11, 13-16]. While pore blocking and constriction could enhance the rejection of some hydrophilic pharmaceuticals by large pore size NF membranes, cake–enhanced concentration polarization (CECP) could occur with smaller pore size membranes causing the opposite effect, i.e. a decrease in rejection [13]. CECP is caused by a reduced back diffusion away from the membrane surface due to the presence of a porous cake layer, which ultimately leads to an even more severe concentration polarization. In addition, organic fouling could interfere with the solute – membrane interaction, and thus hinder diffusive transport of hydrophobic micropollutants through the membrane, resulting in an increase in rejection of such contaminants by NF/RO membranes [11, 16-17]. It is noteworthy that these studies were largely restricted to one particular type of membrane fouling. Thus, it is essential to assess the rejection of micropollutants under various types of membrane fouling.

This study investigated the influence of membrane fouling on the nanofiltration of two PhACs namely – sulfamethoxazole and carbamazepine. Three model foulants were selected in order to represent three distinctive modes of membrane fouling namely organic, organic colloidal, and inorganic colloidal fouling. They were selected in order to simulate organic and colloidal fouling commonly encountered in water recycling applications. The effects of membrane fouling on the rejection of both inorganic salts and pharmaceuticals were examined with respect to the speciation of the compounds and the different modes of membrane fouling. Mechanisms possibly accountable for the effects of membrane fouling on the rejection of PhACs were then proposed and delineated.

2 Materials and Methods

2.1 Nanofiltration membranes

Two nanofiltration (NF) membranes – denoted NF-90 and NF-270 – were used in this investigation. These membranes were supplied by Dow FilmTec (Minneapolis, MN) and were stored dry at 4 ºC. Apart from their difference in membrane pore size, these membranes are quite similar in the physicochemical characteristics (Table 1). According to the manufacturers, both the NF-90 and NF-270 are thin-film composite membranes with a microporous polysulfone supporting layer. The active layers of both the NF-270 and NF-90 membranes contain carboxylic and amine functional groups that can ionize in an aqueous solution, resulting in considerable changes in the membrane surface charge density (measured by the membrane zeta potential) as a function of pH. The average pore sizes of the membranes have been characterized in a previous study by challenging the membranes with a series of inert organic tracers of various molecular weights and applying a pore transport model [18]. The NF-270 was reported to be a "loose" NF membrane, while the NF-90 could be considered as a 'tight' NF membrane.

[TABLE 1]

2.2 Model foulants

Sodium alginate, bovine serum albumin (BSA) and a silica colloid were used as model foulants to simulate hydrophilic organic matter, protein and colloidal particulate matter that are ubiquitous in secondary treated effluent [19-21]. These chemicals were purchased from Sigma Aldrich (Castle Hill, Australia). Molecular weight of the alginate was in the range from 12 to 80 kDa while BSA has a well-defined molecular weight of 67 kDa. The silica colloid (Ludox HS-30) was supplied at 30% suspension in water and was stored in a refrigerator at 4 ºC.

The three model foulants selected in this study have quite distinctive physicochemical properties. The BSA protein has a well defined molecular weight of 67 kDa. It is quite stable, hydrophobic and can behavior like a mono dispersed colloid in an aqueous solution [20]. In the most compacted form, the hydrodynamic dimensions of BSA were in the order of several nanometers [22]. Alginate, on the other hand, is a heterogeneous group of linear water-soluble polysaccharide with molecular weight in the range between 12 and 80 kDa. The alginate

molecule consists of alternating blocks of 1-4 linked α-L-guluronic and β-D-mannuronic acids in various proportions. The α-L-guluronic acid can bind to the divalent cation calcium to form the characteristic egg-box structure [21]. The Ludox HS-30 is a hydrophilic mono-disperse colloidal silica. Zeta potential measurement reported in the literature [23] reveals that the Ludox HS-30 has a very high negative surface charge in comparison to the model organic foulants (Figure 1). It is noteworthy that all model foulants are much larger than the pore sizes of the two membranes used in this study (Table 1). Consequently passage of these model foulants through the membranes was assumed to be negligible and their accumulation on the membrane surface would directly contribute to membrane fouling.

[FIGURE 1]

2.3 Pharmaceutically active compounds

Analytical grade sulfamethoxazole and carbamazepine were purchased from Sigma-Aldrich (Castle Hill, Australia) to represent an ionisable and a neutral pharmaceutical, respectively. These pharmaceutically active compounds are frequently found in secondary treated effluent and sewage impacted water bodies at trace levels. Sulfamethoxazole is one of the most frequently used antibiotics while carbamazepine is a common anti-epileptic drug. The pharmaceuticals were first dissolved in pure methanol to make up stock solutions of 1 g/L. The stock solutions were stored at – 18 ^{o}C and were used within 1 month.

Physicochemical properties of sulfamethoxazole and carbamazepine have been systematically examined in a previous study [6]. Their molecular weights are quite similar to the molecular weight cut-off of nanofiltration membranes (Table 2), which makes them ideal for the comparison and examination of the steric and electrostatic removal mechanisms by the chosen membranes under clean and fouled conditions. The two compounds differ greatly in several parameters, particularly in their speciation behavior. While carbamazepine is uncharged at common pH conditions typical of natural water or wastewater, speciation of sulfamethoxazole is expected in the pH range commonly found in environmental water. The speciation of sulfamethoxazole as a function of the solution pH could dramatically alter the physicochemical properties particularly the electrostatic charge of this compound.

[TABLE 2]

2.4 Other chemicals and reagents

All other chemicals used in this investigation were of analytical grade and were supplied by Sigma-Aldrich (Castle Hill, Australia). Sodium chloride (1 M), calcium chloride (0.1 M), and sodium bicarbonate (0.1 M) were used to prepare the background electrolytes. Adjustment of the feed water pH was carried out with sodium hydroxide (1 M) or hydrochloric acid (1 M). All aqueous solutions used in this investigation were prepared with laboratory grade Milli-Q water.

2.5 Cross flow membrane filtration system

A laboratory-scale, crossflow membrane filtration test unit with a rectangular stainless steel crossflow cell was used. This cell has an effective membrane area of 40 cm^2 (4 cm x 10 cm) with a channel height of 2 mm. The unit utilises a pump (Wanner Engineering Inc., Minneapolis, MN) capable of providing pressures up to 6,800 kPa and a flow rate of 4.2 L/min. The temperature of the test solution was kept constant using a chiller/heater (Neslab RTE 7) equipped with a stainless steel heat exchanging coil submerged directly into the feed reservoir. Permeate flow was measured by a digital flow meter (Optiflow 1000, Agilent Technologies, Palo Alto, CA) connected to a PC, and the cross flow rate was monitored with a rotameter (model 7520, King Instrument Garden Grove, Ca).

2.6 Experimental protocol

The membrane fouling and subsequent rejection experimental protocol was conducted in three steps: compacting, fouling development, and rejection test, as described in a previous study [13]. First, the membrane was compacted using Milli-Q water at 1,800 kPa for at least one hour until a stable baseline flux has been obtained. Fouling layer was then allowed to develop using a foulant cocktail consisting of 20 mg/L of a model foulant in a background electrolyte solution containing 20 mM NaCl, 1 mM $NaHCO_3$, and 1 mM $CaCl_2$. This electrolyte solution was selected to simulate a typical ionic composition of secondary treated effluent. Volume of the feed water solution was 7 liters. Following the addition of the foulants, the crossflow velocity and permeate flux were adjusted to be 30.4 cm/s and 48.5 μm/s (175 $Lm^{-2}h^{-1}$), respectively. This fouling development step was carried out for 18 hours and the feed solution was kept at pH 8.

The accumulation of foulants on the membrane surface was calculated by mass balance assuming negligible back diffusion of these foulants away from the membrane. After the development of the organic fouling layer, the pharmaceutical being examined for the experimental run was spiked to the feed reservoir to make up a concentration of 750 μg/L. The permeate flux was readjusted to be 15 μm/s (54 $Lm^{-2}h^{-1}$) which was similar to the nominal operating permeate fluxes (52 and 41 $Lm^{-2}h^{-1}$ at 480 kPa for the NF-270 and NF-90, respectively) recommended by the manufacturer. The cross-flow velocity was maintained at 30.4 cm/s (representative of cross-flow velocities in spiral-wound elements in full-scale NF/RO plants [24], and corresponding to a feed flow of 90 L/h). The solution pH was raised to approximately pH 10 by addition of a proper volume of 1 M NaOH and the pH was then incrementally dropped to pH 4.0 using stepwise additions 1 M HCl. Prior to sample collection at each pH value, the system was equilibrated for 1 hour. Temperature of the experimental solution was kept constant at 20 ± 0.1 ºC. Both permeate and retentate were recirculated back to the feed reservoir throughout the entire experiment. To examine PhAC rejection by the clean membranes, a similar protocol but without the fouling development step was adapted. Observed rejection is defined as $R = 100\times(1 - C_P/C_F)$, where C_P and C_F are the permeate and the feed concentrations, respectively.

2.7 Contact angle measurement

Contact angle measurement of the clean and fouled membranes was performed with a Rame-Hart Goniometer (Model 250, Rame-Hart, Netcong, NJ) using the standard sessile drop method. MilliQ water was used as the reference liquid. The fouled membranes were air dried prior to the measurement. At least 5 droplets were applied onto duplicate membrane samples and contact angle was measured on both sides of the droplet.

2.8 Analytical methods

A Shimadzu HPLC system (Shimadzu, Kyoto, Japan) equipped with a Supelco Drug Discovery C-18 column (with diameter, length and pore size of 4.6 mm, 150 mm and 5 μm respectively) and UV-Vis detector was used to measure the pharmaceutical concentrations in the feed and permeate. The detection wavelength was 280 nm. The mobile phase used for gradient elution

was milliQ grade deionised water buffered with 0.025 M KH_2PO_4 and acetonitrile, which was delivered at 1 mL/min through the column.

Conductivity and pH were measured using an Orion 4-Star Plus pH/conductivity meter (Thermo Scientific, Beverly, MA, USA).

3 Results and discussion

3.1 Membrane fouling behaviour

A useful approach for better understanding of membrane fouling is to fractionate the foulant constituents of the feed solution into individual components of similar characteristics and systematically study the modes of fouling corresponding to these components [25]. In this study, different modes of fouling were observed using organic (alginate), organic colloidal (BSA) and inorganic colloidal (Ludox HS-30) model foulants. The flux decline profiles of the two NF membranes (as a function of filtration time as well as delivered foulant to the membrane) obtained with feed water containing 20 mg/L of a model foulant in a background electrolyte solution are shown in Figure 2.

[FIGURE 2]

Rapid flux decline occurred immediately after alginate was introduced to the feed solution. After this initial stage of flux decline, the flux decline rate slowed down considerably and a quasi-steady-state fouling layer was fully developed after approximately 18 hours of filtration. As can be seen in Figure 2, flux decline was negligible after 18 hours of filtration despite additional foulant being delivered to the membrane surface. These two fouling stages observed here were probably associated with two separate fouling mechanisms. As the membrane retained most of the alginate, the dominant fouling mechanism occurring initially was probably pore blocking caused by the attachment of the alginate–calcium complex to the membrane surface [26]. This was mostly responsible for the rapid flux decline that occurred until the membrane surface has been covered with approximately 0.5 mg/cm^2 of alginate or the first 2 hours of filtration (Figure 2). Flux decline during the second stage of fouling was mostly attributed to the fouling cake layer thickness and its compaction. In fact, interactions between the alginate molecules in the presence of Ca^{2+} could lead to the formation of large biopolymer aggregates. Under similar

solution chemistry to that used in this study, using dynamic light scattering analysis Li *et al.*, [27] reported that the average aggregate size of alginate was approximately 500 nm. The alginate cake layer was therefore much more porous than the membrane active polymeric layer. Consequently, further delivery of alginate to the membrane surface beyond this point only resulted in a negligible flux decline. Alginate fouling was slightly more severe for the large pore size NF-270 membrane in comparison to the tight NF-90 membrane (Figure 2). The presented data confirmed a good experimental reproducibility when alginate was used as a model foulant. The fouling profiles of repeated filtration tests under the same experimental condition were almost identical.

While good reproducibility was also obtained with BSA fouling, it is noteworthy that the fouling profile caused by BSA was rather different from that caused by alginate. The permeate flux decline was linearly proportional to the amount of BSA being delivered to the membranes without any sign of reaching a steady-state flux. In an aqueous solution, BSA could behavior as a hydrophobic and monodispersed biocolloid with an effective hydrodynamic diameter of 7 – 8 nm. Hydrophobic interactions between BSA molecules could possibly lead to the formation of a compacted and colloidal–like cake layer, causing considerable flux decline as a result of an increase in hydraulic resistance and more importantly the cake enhanced osmotic pressure effect. This premise is supported by contact angle measurement data, which show a remarkable increase in surface hydrophobicity when the membranes were fouled with BSA (Figure 3).

[FIGURE 3]

Fouling experiments conducted with the Ludox HS-30 silica colloid show a typical colloidal fouling behaviour (Figure 2). Membrane fouling caused by the silica colloid Ludox-HS was considerably less severe than that caused by the model organic foulant alginate. The reproducibility of colloidal fouling experiments was quite poor which could possibly be attributed to a weak adhesive force between these colloidal particles. It is noteworthy that in a suspended aqueous solution, the Ludox-HS has a very high negative charge. Contact angle measurement also confirms a very hydrophilic colloidal cake layer on the membrane surface (Figure 3).

The three distinctive modes of membrane fouling appear to result in quite different overall flux decline after 18 hours of filtration. Within the first 18 hours of filtration, organic fouling caused by alginate resulted in the most severe membrane fouling while silica colloidal fouling by the Ludox-HS led to the least flux decline. Due to the formation of a colloidal–like cake layer, intermediate flux decline was observed as the membranes were fouled with the protein BSA. The three modes of membrane fouling observed here could also affect solute rejection in quite different ways as will be discussed in the next section.

3.2 Salt rejection under different modes of membrane fouling

The influence of membrane fouling on the rejection of inorganic salts was examined by comparing conductivity rejection data under clean and fouled conditions at the same permeate flux (Figure 4). The NF-90 membrane previously fouled with either model foulants consistently showed a slightly lower but nevertheless discernible salt rejection in comparison to the clean condition, whereas the effects of membrane fouling on salt rejection by the NF-270 membrane were quite remarkable. It is noteworthy that the NF-90 and NF-270 membranes differ significantly in their average pore sizes. The NF-90 is a tight nanofiltration membrane with a small average pore size of 0.68 nm in diameter. Consequently, steric hindrance (or size exclusion) is expected to play a major role governing the separation process by this. On the other hand, both steric hindrance and electrostatic interaction can be relevant mechanisms in the separation of inorganic salts by the loose NF-270 membrane. A decrease in the solution pH can also result in a decrease in the membrane surface charge density. Consequently, electrostatic interaction between ionic species and the membrane surface diminished resulting in a remarkable drop in conductivity rejection by the clean NF-270 membrane as the solution pH decrease. In the presence of all three model foulants, the solution pH exerts a much lesser influence on conductivity rejection by the fouled NF-270 membrane as compared to that by the virgin (clean) NF-270 membrane (Figure 4a).

[FIGURE 4]

Overall, the effects of fouling on inorganic salt rejection were consistent with the three modes of membrane fouling. Although alginate caused the most severe fouling, the influence of alginate fouling on inorganic salt rejection was small. At high pH, alginate fouling led to a discernible

reduction in conductivity rejection while at less than pH 6, a small improvement in conductivity rejection could be observed. It is possible that pore blocking caused by small alginate molecules could improve rejection to some extent. The effect of pore blocking could not be seen at high pH possibly due to strong electrostatic interaction between ionic species and the membrane surface as delineated above. In contrast, the influence of colloidal fouling on conductivity rejection was quite dramatic even though flux decline caused by silica colloid was the least severe. The influence of protein fouling on conductivity rejection was intermediate between alginate and colloid fouling. BSA has an isoelectric point at pH 4.7 [22] and can become positively charged at pH 4. As a result, the small increase in conductivity rejection by the BSA fouled NF-270 membrane at pH 4 could also be attributed to an enhanced electrostatic interaction (Figure 4a). It is noteworthy that when the NF-270 was fouled with colloidal silica, conductivity rejection was dramatically reduced to almost zero. Although the colloidal silica used in this study is highly negatively charged (Figure 1), it is noteworthy that the average diameter of these particles is about 16 nm. Consequently, when packed closely, these particles will result in a porous cake layer. Since the range of electrostatic force is typically less than a nanometer, the increase in the negative surface charge as a result of colloidal fouling would not result in any discernible influence on the rejection of charged solutes. In fact, the remarkable reduction in conductivity rejection due to colloidal fouling could be attributed to the 'cake-enhanced concentration polarisation'. This was consistent with the mechanism of colloidal fouling discussed in the previous section. Elimelech and co-workers demonstrated that the fouling cake layer could hinder back diffusion of solutes to the bulk solution, hence causing solute to accumulate near the membrane surface [28-29]. This CECP resulted in greater concentration gradient across the membrane and subsequently a decrease in solute rejection as can be seen for both the NF-270 and NF-90 membranes (Figure 4). However, it was also reported that cake-enhanced concentration polarisation cause a much lesser reduction in rejection when the membrane was fouled by organic instead of inorganic colloidal matter [29].

3.3 PhACs rejection under different modes of membrane fouling

In our previous study using humic acid as a model foulant, it was demonstrated that the influence of membrane fouling on the rejection of PhACs decreased as the membrane pore size decreased [13]. A similar observation could be made in this study using three other model foulants. Figure

5 shows the rejection of sulfamethoxazole under clean and fouled conditions at solution pH in the range between pH 4 and pH 10. Because the NF-90 is a tight nanofiltration filtration membrane with pore size smaller or comparable to the three pharmaceuticals investigated here, rejection of sulfamethoxazole by this membrane under both clean and fouled conditions was close to 100% (Figure 5b). A very small but nevertheless consistent and discernible decrease in sulfamethoxazole rejection by the NF-90 membranes previously fouled with alginate, BSA and silica colloid could still be observed at low pH (Figure 5b).

[FIGURE 5]

In contrast, membrane fouling showed a significant effect on the rejection of sulfamethoxazole by the loose NF-270 membrane. Possessing a sulfonamine functional group with a pK_a value of 5.7, sulfamethoxazole can be deprotonated as thus can exist as both negatively charged and neutral species in an aqueous solution depending on the solution pH. Consequently, the speciation of sulfamethoxazole as a function of the solution pH has a notable effect on rejection of this compound by the loose NF-270 membrane under both clean and fouled conditions (Figure 5a). Sulfamethoxazole rejection by the NF-270 membrane varied significantly as the solution pH was reduced from pH 10 to pH 4. However, the rejection curves for both clean and fouled membranes closely resemble the speciation of the compound in this pH range. Once again, it is interesting to note that the influence of membrane fouling on the rejection of sulfamethoxazole appears to be strongly foulant dependent. A remarkable reduction in rejection was observed with colloidal fouling while alginate and protein fouling also caused a small but clearly discernible drop in sulfamethoxazole rejection. It is evident that cake-enhanced concentration polarisation is primarily responsible for the large reduction in sulfamethoxazole by the NF-270 membrane under colloidal fouling condition. On the other hand, it is noted that concentration polarization caused by aliginate and BSA fouling would be considerably less than that caused by inorganic colloidal fouling [29]. Furthermore, pore blocking caused by small alginate molecules could improve rejection and thus counter balance the impact of CECP to some extent. Therefore, while the additional hydraulic resistance caused by alginate and protein fouling led to more severe flux decline, organic fouling exerted a lesser impact on the rejection of sulfamethoxazole.

Consistent with previous results, the NF-90 membrane showed near complete rejection of carbamazepine under both clean and fouled conditions (Figure 6b). The effects of membrane fouling on the rejection of carbamazepine by this membrane were rather inconclusive. However, a clear connection between the effects of membrane fouling on rejection and modes of fouling could be observed with the loose NF-270 membrane (Figure 6a). Lowest rejection value was obtained when the membrane was fouled with silica colloid. Rejection of carbamazepine by the alginate and protein fouled NF-270 membranes was considerably lower than that under clean membrane condition. Unlike sulfamethoxazole, carbamazepine could only exist as a neutral species in the entire pH range being examined and the separation of this compound was probably governed solely by size exclusion (or steric hindrance). As a result, there was no significant variation in carbamazepine rejection as solution pH varied from pH 10 to pH 4. A somewhat considerable drop in rejection at pH near or below the isoelectric point of BSA (pH 4.7) by the NF-270 previously fouled with a BSA solution could be attributed to conformation change of the protein macromolecule into a more compacted and colloidal form as this protein became neutrally charged. Once again, the phenomenon observed here could be explained by the CECP effect which was more prominent with colloidal fouling.

[FIGURE 6]

4 Conclusion

The influence of membrane fouling on solute rejection by the tight nanofiltration NF-90 membrane was negligible. On the other hand, remarkable effects of membrane fouling on the rejection of both inorganic salts and PhACs were observed with the loose nanofiltration NF-270 membrane. These effects could be attributed to the cake enhanced concentration polarization. It is noteworthy that such effects were strongly foulant–dependent. The three foulants used in this study resulted in three distinctive modes of membrane fouling. Subsequently, these three modes of membrane fouling consistently showed different effects on the membrane separation efficiency. Inorganic colloidal fouling caused the most severe rejection decrease even though this form of membrane fouling only resulted in a small flux decline. This reduction in rejection was attributed to a strong cake-enhanced concentration polarization (CECP) effect which was also the primary mechanism of flux decline in inorganic colloidal fouling. In contrast, organic fouling caused by the model foulant alginate led to a much lesser decrease in the rejection of PhACs

despite the fact that alginate caused the most severe flux decline. CECP caused by alginate fouling was less severe than that by the silica colloids used in this study. In addition, it is also possible that pore blocking caused by small alginate molecules could improve rejection and thus lessen the impact of cake-enhanced concentration polarization. The influence of fouling on rejection as well as the extent of membrane fouling caused by the protein BSA was intermediate between silica colloidal and alginate fouling.

5 References

[1] M.A. Shannon, P.W. Bohn, M. Elimelech, J.G. Georgiadis, B.J. Marinas, and A.M. Mayes, Science and technology for water purification in the coming decades. *Nature*, **452**(7185) (2008): p. 301-310.

[2] T. Fujioka, S.J. Khan, Y. Poussade, J.E. Drewes, and L.D. Nghiem, N-nitrosamine removal by reverse osmosis for indirect potable water reuse – A critical review based on observations from laboratory-, pilot- and full-scale studies. *Sep. Purif. Technol.*, **98** (2012): p. 503-515.

[3] R.P. Schwarzenbach, B.I. Escher, K. Fenner, T.B. Hofstetter, C.A. Johnson, U. von Gunten, and B. Wehrli, The challenge of micropollutants in aquatic systems. *Science*, **313**(5790) (2006): p. 1072-1077.

[4] X. Jin, J. Hu, and S.L. Ong, Influence of dissolved organic matter on estrone removal by NF membranes and the role of their structures. *Water Res.*, **41**(14) (2007): p. 3077.

[5] L.D. Nghiem, A. Manis, K. Soldenhoff, and A.I. Schafer, Estrogenic hormone removal from wastewater using NF/RO membranes. *J. Membr. Sci.*, **242**(1-2) (2004): p. 37.

[6] L.D. Nghiem, A.I. Schäfer, and M. Elimelech, Pharmaceutical Retention Mechanisms by Nanofiltration Membranes. *Environ. Sci. Technol.*, **39**(19) (2005): p. 7698-7705.

[7] T. Fujioka, L.D. Nghiem, S.J. Khan, J.A. McDonald, Y. Poussade, and J.E. Drewes, Effects of feed solution characteristics on the rejection of N-nitrosamines by reverse osmosis membranes. *J. Membr. Sci.*, **409-410** (2012): p. 66-74.

[8] L.D. Nghiem, A.I. Schaffer, and M. Elimelech, Nanofiltration of hormone mimicking trace organic contaminants. *Sep. Sci. Technol.*, **40**(13) (2005): p. 2633-2649.

[9] C. Bellona, J.E. Drewes, P. Xu, and G. Amy, Factors affecting the rejection of organic solutes during NF/RO treatment - a literature review. *Water Res.*, **38**(12) (2004): p. 2795-2809.

[10] A.I. Schäfer, N. Andritsos, A.J. Karabelas, E.M.V. Hoek, R. Scheider, and M. Nyström, *Fouling in nanofiltration*, in *Nanofiltraiton - Principles and Applications*, A.I. Schäfer, D. Waite, and A. Fane, Editors. 2005, Elservier: New York. p. 169–239.

[11] P. Xu, J.E. Drewes, T.-U. Kim, C. Bellona, and G. Amy, Effect of membrane fouling on transport of organic contaminants in NF/RO membrane applications. *J. Membr. Sci.*, **279**(1-2) (2006): p. 165.

[12] D. Vogel, A. Simon, A.A. Alturki, B. Bilitewski, W.E. Price, and L.D. Nghiem, Effects of fouling and scaling on the retention of trace organic contaminants by a nanofiltration membrane: The role of cake-enhanced concentration polarisation. *Sep. Purif. Technol.*, **73**(2) (2010): p. 256-263.

[13] L.D. Nghiem and S. Hawkes, Effects of membrane fouling on the nanofiltration of pharmaceutically active compounds (PhACs): Mechanisms and role of membrane pore size. *Sep. Purif. Technol.*, **57**(1) (2007): p. 176.

[14] M.J. López-Muñoz, A. Sotto, J.M. Arsuaga, and B. Van der Bruggen, Influence of membrane, solute and solution properties on the retention of phenolic compounds in aqueous solution by nanofiltration membranes. *Sep. Purif. Technol.*, **66**(1) (2009): p. 194-201.

[15] K.L. Tu, A.R. Chivas, and L.D. Nghiem, Effects of membrane fouling and scaling on boron rejection by nanofiltration and reverse osmosis membranes. *Desalination*, **279**(1-3) (2011): p. 269-277.

[16] T. Fujioka, S.J. Khan, J.A. McDonald, R.K. Henderson, Y. Poussade, J.E. Drewes, and L.D. Nghiem, Effects of membrane fouling on N-nitrosamine rejection by nanofiltration and reverse osmosis membranes. *J. Membr. Sci.*, **427** (2013): p. 311-319.

[17] L.D. Nghiem and P.J. Coleman, NF/RO filtration of the hydrophobic ionogenic compound triclosan: Transport mechanisms and the influence of membrane fouling. *Sep. Purif. Technol.*, **62**(3) (2008): p. 709-716.

[18] L.D. Nghiem, A.I. Schäfer, and M. Elimelech, Removal of Natural Hormones by Nanofiltration Membranes: Measurement, Modeling, and Mechanisms. *Environ. Sci. Technol.*, **38** (2004): p. 1888-1896.

[19] K. Boussu, A. Belpaire, A. Volodin, C. Van Haesendonck, P. Van der Meeren, C. Vandecasteele, and B. Van der Bruggen, Influence of membrane and colloid characteristics on fouling of nanofiltration membranes. *J. Membr. Sci.*, **289**(1-2) (2007): p. 220.

[20] W.S. Ang and M. Elimelech, Protein (BSA) fouling of reverse osmosis membranes: Implications for wastewater reclamation. *J. Membr. Sci.*, **296**(1-2) (2007): p. 83.

[21] W.S. Ang, S. Lee, and M. Elimelech, Chemical and physical aspects of cleaning of organic-fouled reverse osmosis membranes. *J. Membr. Sci.*, **272**(1-2) (2006): p. 198.

[22] M.L. Ferrer, R. Duchowicz, B. Carrasco, J.G. de la Torre, and A.U. Acuna, The conformation of serum albumin in solution: A combined phosphorescence depolarization-hydrodynamic modeling study. *Biophys. J.*, **80**(5) (2001): p. 2422-2430.

[23] K. Boussu, A. Belpaire, A. Volodin, C. Van Haesendonck, P. Van der Meeren, C. Vandecasteele, and B. Van der Bruggen, Influence of membrane and colloid characteristics on fouling of nanofiltration membranes. *J. Membr. Sci.*, **289**(1-2) (2007): p. 220-230.

[24] A.R.D. Verliefde, E.R. Cornelissen, S.G.J. Heijman, I. Petrinic, T. Luxbacher, G.L. Amy, B. Van der Bruggen, and J.C. van Dijk, Influence of membrane fouling by (pretreated) surface water on rejection of pharmaceutically active compounds (PhACs) by nanofiltration membranes. *J. Membr. Sci.*, **330**(1-2) (2009): p. 90-103.

[25] H.K. Shon, S. Vigneswaran, I.S. Kim, J. Cho, and H.H. Ngo, Fouling of ultrafiltration membrane by effluent organic matter: A detailed characterization using different organic fractions in wastewater. *J. Membr. Sci.*, **278**(1-2) (2006): p. 232-238.

[26] G.T. Grant, E.R. Morris, D.A. Rees, P.J.C. Smith, and D. Thom, Biological interactions between polysaccharides and divalent cations: The egg-box model. *FEBS Lett.*, **32**(1) (1973): p. 195-198.

[27] Q. Li, Z. Xu, and I. Pinnau, Fouling of reverse osmosis membranes by biopolymers in wastewater secondary effluent: Role of membrane surface properties and initial permeate flux. *J. Membr. Sci.*, **290**(1-2) (2007): p. 173-181.

[28] H.Y. Ng and M. Elimelech, Influence of colloidal fouling on rejection of trace organic contaminants by reverse osmosis. *J. Membr. Sci.*, **244**(1-2) (2004): p. 215-226.

[29] S. Lee, J. Cho, and M. Elimelech, Combined influence of natural organic matter (NOM) and colloidal particles on nanofiltration membrane fouling. *J. Membr. Sci.*, **262**(1-2) (2005): p. 27-41.

[30] P. Xu, J.E. Drewes, T.-U. Kim, C. Bellona, and G. Amy, Effect of membrane fouling on transport of organic contaminants in NF/RO membrane applications. *J. Membr. Sci.*, **279**(1-2) (2006): p. 165-175.

[31] D. Kuzmenko, E. Arkhangelsky, S. Belfer, V. Freger, and V. Gitis, Chemical cleaning of UF membranes fouled by BSA. *Desalination*, **179**(1-3) (2005): p. 323-333.

Table 1: Properties of the selected NF membranes

Membrane	Pure water permeability ($Lm^{-2}h^{-1}bar^{-1}$)	Average pore diameter (nm)	Contact Angle (^{o})	NaCl rejection (%)
NF-270	13.5	0.84	23.4	40
NF-90	6.4	0.68	42.5	85

Table 2: Intrinsic physicochemical properties of pharmaceuticals.

	Sulfamethoxazole	Carbamazepine
Molecular weight (g/mol)	253.3	236.3
Molecular width[a] (nm)	0.526	0.507
Molecular height[a] (nm)	0.587	0.529
Molecular length[a] (nm)	1.031	0.891
Log K_{OW} [b]	0.89	2.45
Dissociation constant[b]	pK_{a1} = 1.4, pK_{a2} = 5.8	pK_a = 2.3
Molecular structure	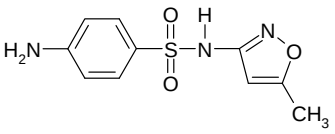	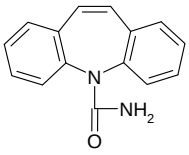

[a] Ref: Calculated using ChemOffice 2005.

[b] Ref: SciFinder Scholar, data calculated using Advanced Chemistry Development (ACD/Labs) Software V8.14 for Solaris (1994–2007 ACD/Labs).

FIGURE CAPTIONS

Figure 1. (A) – Zeta potential of the NF-270 and NF-90 membranes and (B) – Zeta potential of the model foulants (Data from [6, 23, 30-31]).

Figure 2. Normalised permeate flux of the NF-270 and NF-90 membranes as a function of filtration time (top) and delivered alginate (bottom) (Feed solution: 1mM of $NaHCO_3$, 20 mM of NaCl, 1 mM of $CaCl_2$, and 20 mg/L of a model foulant, pH = 8; error bars show the standard deviation of 2 or 3 repetitive experiments).

Figure 3. Change in membrane surface hydrophobicity due to fouling of the NF-270 and NF-90 membranes. Experimental conditions are as in caption of Figure 2.

Figure 4. Conductivity rejection by the (a) NF-270 and (b) NF-90 membranes under clean and fouled conditions as a function of pH.

Figure 5. Sulfamethoxazole rejection by the (a) NF-270 and (b) NF-90 membranes under clean and fouled conditions as a function of pH.

Figure 6. Carbamazepine rejection by the (a) NF-270 and (b) NF-90 membranes under clean and fouled conditions as a function of pH.

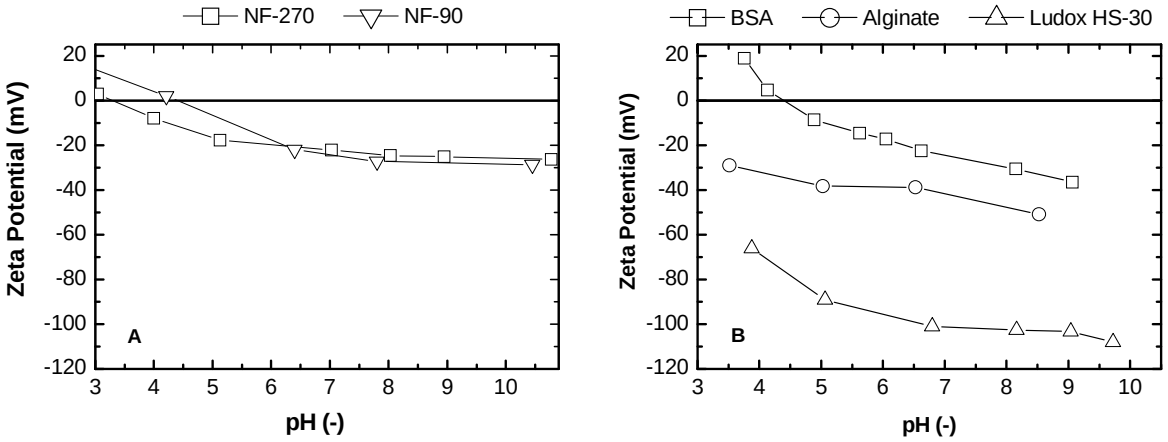
NF-270
NF-90
Zeta Potential (mV)
pH (-)
A
BSA
Alginate
Ludox HS-30
Zeta Potential (mV)
pH (-)
B

FIGURE 1

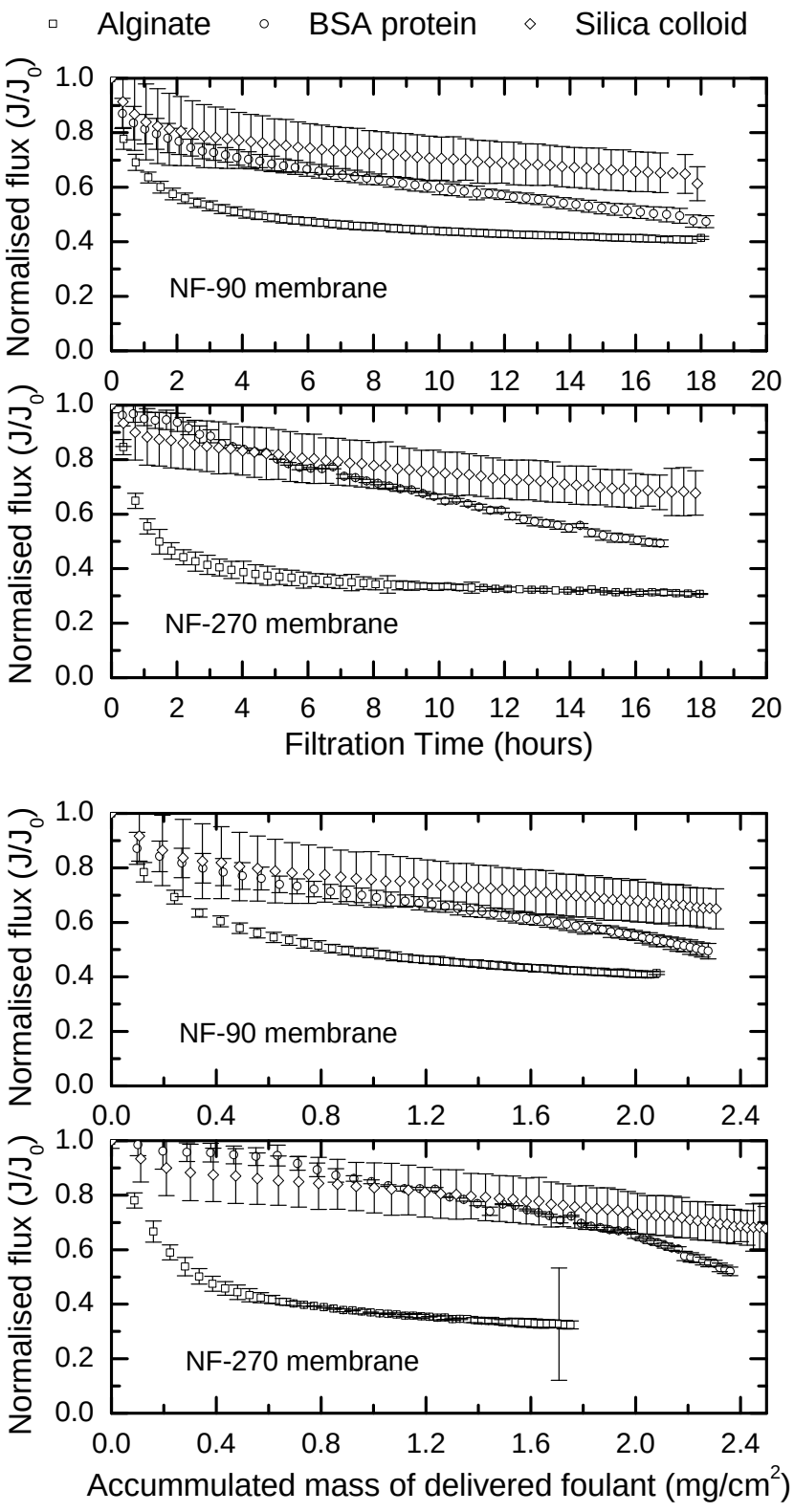
Alginate
BSA protein
Silica colloid
Normalised flux (J/J0)
NF-90 membrane
NF-270 membrane
Filtration Time (hours)
Accummulated mass of delivered foulant (mg/cm2)

FIGURE 2

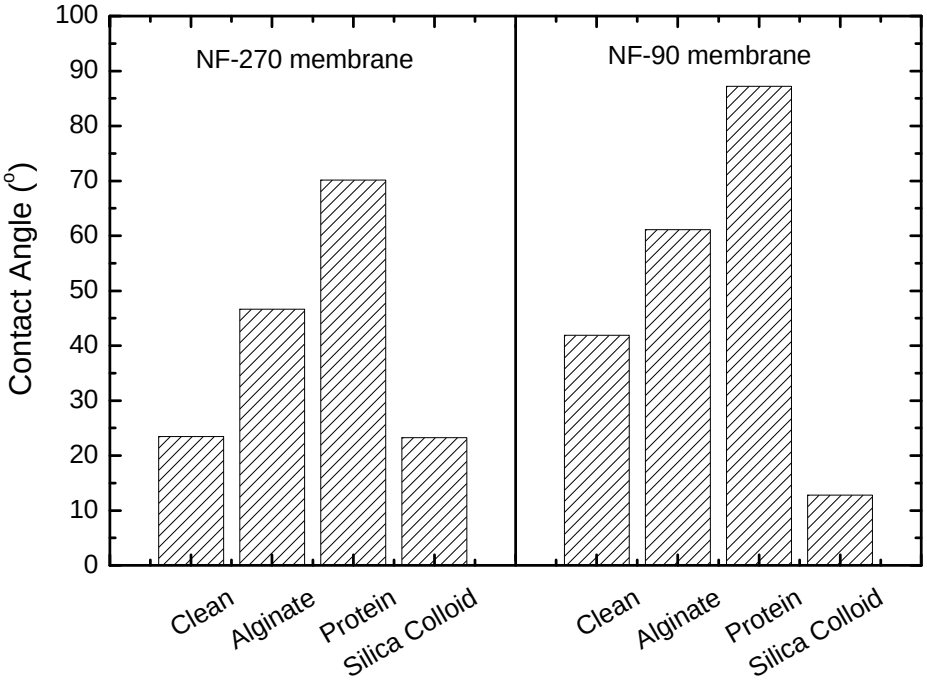
Contact Angle (°)
100
90
80
70
60
50
40
30
20
10
0
NF-270 membrane
NF-90 membrane
Clean
Alginate
Protein
Silica Colloid
Clean
Alginate
Protein
Silica Colloid

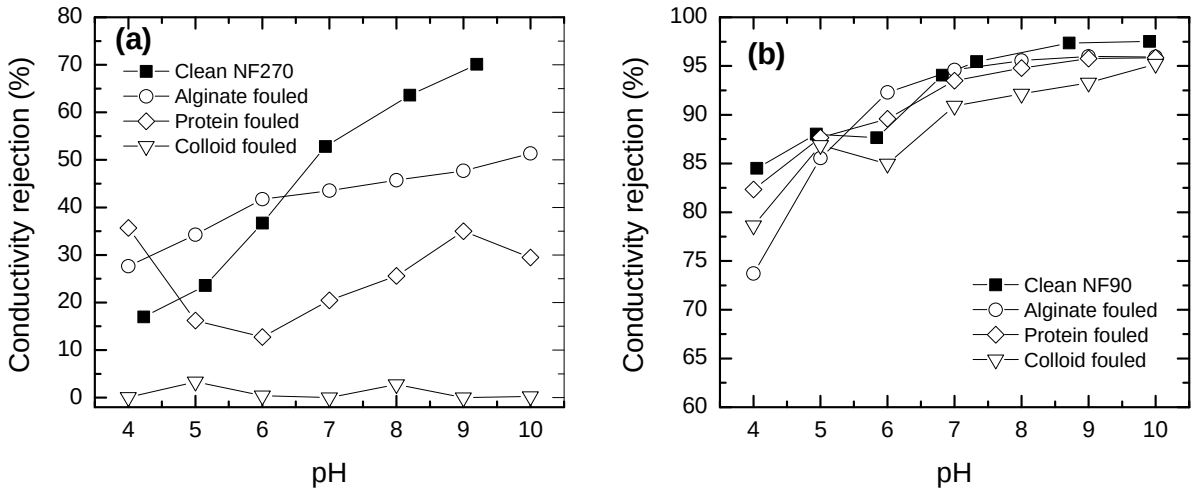
(a)
Clean NF270
Alginate fouled
Protein fouled
Colloid fouled
Conductivity rejection (%)
pH
(b)
Clean NF90
Alginate fouled
Protein fouled
Colloid fouled
Conductivity rejection (%)
pH

FIGURE 4

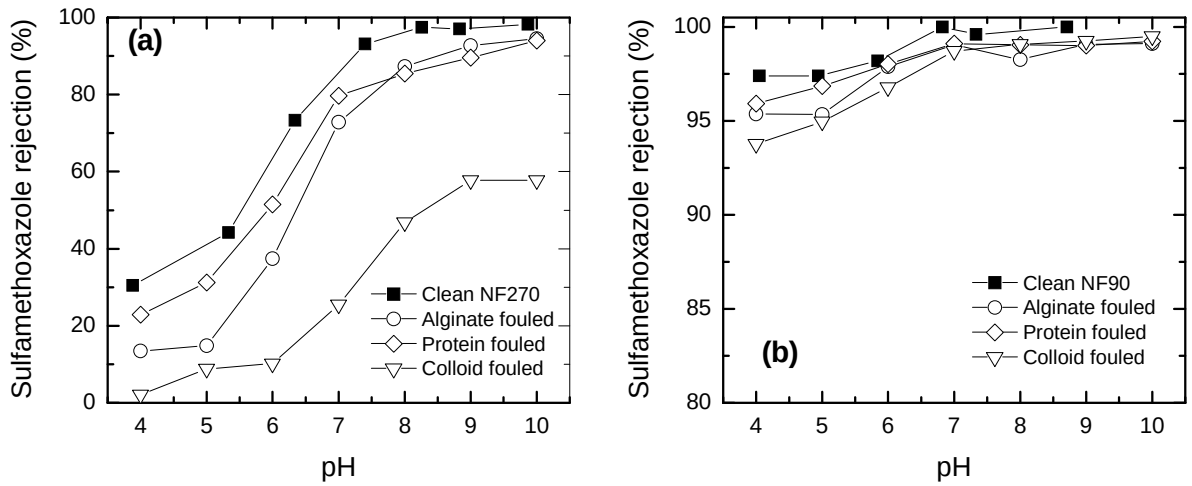
(a)
Sulfamethoxazole rejection (%)
pH
Clean NF270
Alginate fouled
Protein fouled
Colloid fouled
(b)
Clean NF90
Alginate fouled
Protein fouled
Colloid fouled

FIGURE 5

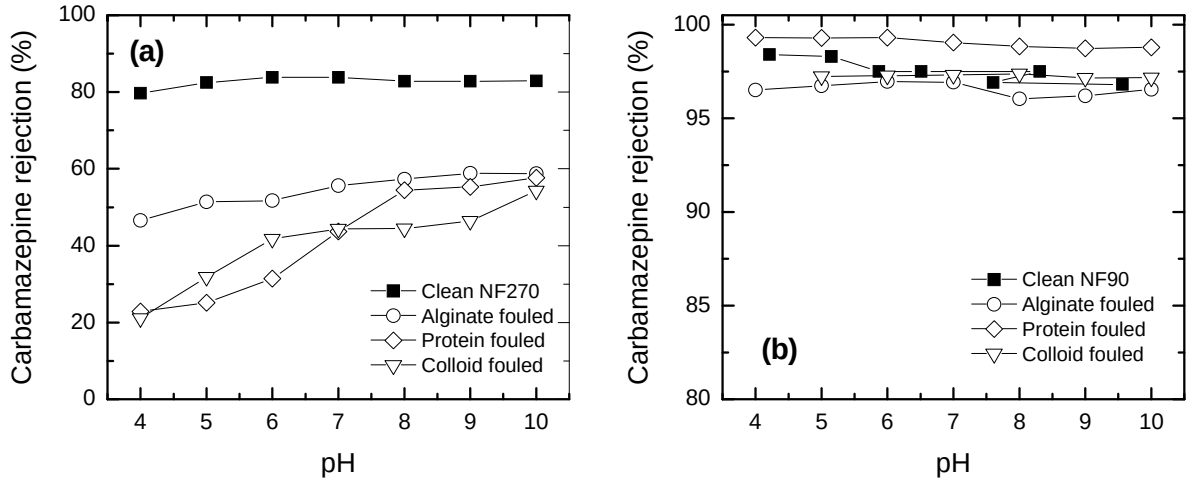
(a)
Carbamazepine rejection (%)
pH
Clean NF270
Alginate fouled
Protein fouled
Colloid fouled
(b)
Carbamazepine rejection (%)
pH
Clean NF90
Alginate fouled
Protein fouled
Colloid fouled

FIGURE 6